Development of Transmitter and Receiver With Set Partitioning 64APSK Coded Modulation Designed on Basis of Channel Capacity

Yuki Koizumi, *Member, IEEE*, Yoichi Suzuki, *Member, IEEE*, Masaaki Kojima, *Member, IEEE*, Kazunori Yokohata, and Hisashi Sujikai

***Abstract*—In this paper, we present a prototype transmitter and receiver with set partitioning (SP)-64 amplitude and phase shift keying (APSK) coded modulation we developed for expanding satellite transmission capacity. SP-multi-level coded modulation is a transmission scheme that can improve noise immunity by properly combining a modulation scheme, bit allocation, and error-correction codes. We designed SP-64APSK coded modulation on the basis of channel capacity for expanding satellite transmission capacity. We confirmed that it has higher robustness to additive white Gaussian noise (AWGN) than DVB-S2X's 64APSK modulation with Gray mapping through computer simulation. We also developed a prototype transmitter and receiver to implement our SP-64APSK coded modulation and evaluated its transmission performances in an AWGN channel and in a non-linear channel simulating 12-GHz-band satellite transponder characteristics. We describe the method of designing our SP-64APSK coded modulation through computer simulation, the modulation/demodulation process, and transmission performances of the prototype transmitter and receiver. We also indicate that 8K ultra-high definition television (UHDTV) with an encoded bit rate of 150 Mbps can be transmitted using the prototype within 34.5 MHz, which is the bandwidth of a single transponder for satellite broadcasting in Japan.**

***Index Terms*—64APSK, coded modulation, set partitioning, channel capacity, 4K/8K, UHDTV, satellite transmission.**

I. Introduction

COMMERCIAL satellite broadcasting of 4K/8K ultra-high definition television (UHDTV) [1], [2] was launched in December 2018 in Japan [3]. Its transmission system is ISDB-S3 [4]–[6], which can broadcast one 8K program or three 4K programs in the same bandwidth (34.5 MHz) as current HDTV satellite broadcasting. The required transmission capacity of 100 Mbps for 4K/8K UHDTV satellite broadcasting is achieved by setting the transmission parameters to a symbol rate of 33.7561 Mbaud, roll-off factor of 0.03, using a 16 amplitude and phase shift keying (APSK) modulation scheme, and low-density parity-check (LDPC) coding rate of 7/9.

Japan Broadcasting Corporation (NHK) has been researching more realistic and immersive video/audio systems for new broadcasting services, e.g., a full-featured 8K system with a high frame rate of 120 Hz [7], augmented reality/virtual reality system, and viewable three-dimensional television without special glasses. Satellite broadcasting will play an important role in transmitting such new services to the home, but it is necessary to increase its transmission capacity because these services will require faster data rates than those of current UHDTV services. One way to increase the capacity is to adopt a higher multi-level modulation scheme. Since the ISDB-S3 system used in Japan's UHDTV satellite broadcasting supports a maximum of 32APSK, we designed a new 64APSK-scheme. However, the higher the order of the modulation scheme, the more susceptible it is to noise. Therefore, we aimed for a more robust transmission-to-noise than 64APSK with Gray mapping by applying set partitioning (SP)-multi-level coded modulation [8] to design a new 64APSK.

SP-coded modulation is a classical technique and many studies have been devoted to improving the performance of multi-level modulation. Isaka *et al.* [9] proposed asymmetric 8 phase shift keying (PSK) and 16 quadrature amplitude modulation (QAM) coded modulations with unconventional SP different from the Ungerboeck-type. Farhoudi and Rusch [10] evaluated the performance of the SP-16QAM coded modulation optimized for non-linear phase noise in a coherent system. Tanahashi and Ochiai [11] reported on the SP-coded modulation with hexagonal shell modulation, which has a lower peak-to-average power ratio than a standard QAM.

We have been engaged in further expansion of transmission capacity with SP-multi-level coded modulations as a next-generation satellite broadcast system [12]–[16]. In this paper, we propose the SP-64APSK coded modulation with coding rate of 4/5, by which the maximum bit rate of ISDB-S3 is exceeded, designed on the basis of channel capacity and describe the performance evaluation of a prototype transmitter and receiver implementing this modulation.

This paper is structured as follows. In Section II, we give an overview of SP-multi-level coded modulation. In Section III, we describe the SP-64APSK coded modulation design method

Manuscript received 10 September 2021; revised 27 December 2021 and 11 April 2022; accepted 25 April 2022. Date of publication 24 May 2022; date of current version 5 September 2022. *(Corresponding author: Yuki Koizumi.)*

Yuki Koizumi, Masaaki Kojima, and Hisashi Sujikai are with the Science and Technology Research Laboratories, NHK, Tokyo 157-8510, Japan (e-mail: koizumi.y-hq@nhk.or.jp; kojima.m-iw@nhk.or.jp; sujikai.h-dy@nhk.or.jp).

Yoichi Suzuki is with the Engineering Administration, NHK, Tokyo 157-8510, Japan (e-mail: suzuki.y-fw@nhk.or.jp).

Kazunori Yokohata is with the Asahikawa Station, NHK, Asahikawa 070-8680, Japan (e-mail: yokohata.k-jm@nhk.or.jp).

Digital Object Identifier 10.1109/TBC.2022.3176190

on the basis of channel capacity through computer simulation. We first define the channel capacity then explain the constellation design, SP-applicable bit allocation, and error-correction code design. In Section IV, we describe our prototype transmitter and receiver implementing our designed SP-64APSK coded modulation (hereafter called prototype). We present the specifications of the prototype and explain the modulation/demodulation and multi-level decoding process, which repeats symbol division and error-correction decoding. In Section V, we discuss the transmission performance of the prototype in an additive white Gaussian noise (AWGN) channel and non-linear channel simulating 12-GHz-band satellite transponder characteristics then present the results of an 8K UHDTV transmission experiment with our prototype. We conclude the paper in Section VI.

II. Overview of SP-Multi-Level Coded Modulation

SP-multi-level coded modulation is a transmission scheme that can improve noise immunity by properly combining a modulation scheme, bit allocation, and error-correction coding. It can extend the minimum Euclidean distance (D_{min}) between constellation symbols by dividing them in accordance with the decoding result of each bit. The combination of SP and the design of appropriate error-correction codes for symbol division provides high robustness against noise.

Transmission schemes with Gray mapping, where the Hamming distance between adjacent symbols is 1, are widely used. Focusing on the bit error rate (BER) for each bit allocated to their symbols, these BER characteristics are non-uniform due to multi-level/multi-phase modulation schemes. Therefore, applying a single error-correction code to the bit streams mapped to those symbols causes transmission performance degradation. Bit-interleaved coded modulation (BICM) [17], [18], which is the modulation method to reduce the non-uniformity with bit-interleave before mapping, is effective in mitigating such degradation. The transmission scheme combining BICM and Gray mapping is widely used in actual satellite transmission systems, e.g., ISDB-S3 [4]–[6] and DVB-S2X [19]. Transmission performance can be improved by further reducing the non-uniformity. SP-coded modulation is a means to achieve this because it is a scheme that applies appropriate error-correction codes to bit streams with the non-uniformity of the BER characteristics for each bit. The bit sequence allocated to a constellation symbol is decoded bit by bit, and the constellation symbols are divided in accordance with the decoding results for each bit. It enables to extend D_{min} as the decoding progresses. Therefore, by designing error-correcting codes with an appropriate capability in accordance with the D_{min} of each decoding stage, better transmission performance can be achieved than with a transmission scheme that combines BICM and Gray mapping.

Taking SP-8PSK coded modulation as an example, Fig. 1 illustrates the set-partitioning process for SP-coded modulation constellations and the relationship between SP-applicable bit allocation and expansion of D_{min}. Three-bit (a1, a2, a3) allocation to the 8PSK constellation is SP-applicable

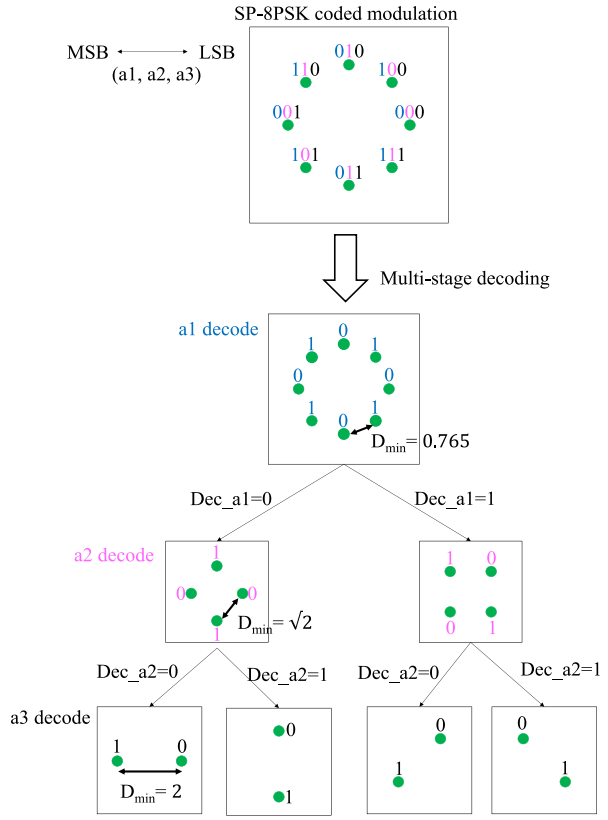

Fig. 1. Set-partitioning process for a SP-8PSK coded modulation constellation.

mapping, and let a1 and a3 be the most significant bit (MSB) and least significant bit (LSB), respectively. The 8PSK constellation is divided into two quadrature phase shift keying (QPSK) constellations on the basis of a1, and each QPSK constellation is further divided into two binary phase shift keying (BPSK) constellations on the basis of a2. Therefore, we have four BPSK constellations in accordance with a1 and a2. SP-8PSK coded modulation signals are decoded in the order of a1, a2, and a3 by a multi-stage decoding process. First, a1 is decoded in the 8PSK constellation. Next, a2 is decoded in the QPSK constellation in accordance with the decoded a1 (Dec_a1 = 0 or 1). Finally, a3 is decoded in the BPSK constellation in accordance with the decoded a2 (Dec_a2 = 0 or 1).

As the decoding stage progresses, robustness against bit errors increases due to the increase in D_{min}. This means that bit sequences consisting of bits closer to LSB can be transmitted in a higher coding rate with fewer parity bits. Therefore, overall transmission performance can be improved with SP-multi-level coded modulation by applying the appropriate error-correction coding rate to each bit in accordance with the D_{min} in each decoding stage.

III. Design of 64APSK Coded Modulation

The design of SP-multi-level coded-modulation mainly consists of designs of constellation, bit allocation, and error-correction code. In this section, we discuss the design method through computer simulation consisting of the above design

methods for our SP-64APSK coded modulation. The constellation and bit allocation are designed to extend D_{min} on the base of channel capacity T [20] (described in Section III-A). The LDPC code is applied as an error-correction code, and the coding rate is individually adjusted to improve the overall transmission performance in accordance with the BER characteristics of each bit before error correction.

A. Definition of Channel Capacity

T is the upper bound on the information rate that can be transmitted with as low an error rate as possible in the arbitrary transmission path. Let $\boldsymbol{X}$ and $\boldsymbol{Y}$ be the transmitted and received symbols, respectively. The mutual information between $\boldsymbol{X}$ and $\boldsymbol{Y}$ is expressed as $I(\boldsymbol{X};\boldsymbol{Y})$, and T is the maximum of $I(\boldsymbol{X};\boldsymbol{Y})$ when $p(\boldsymbol{X})$, the probability distribution of occurrence of $\boldsymbol{X}$, is changed, which is

$$T = \max_{p(\boldsymbol{X})} I(\boldsymbol{X};\boldsymbol{Y}), \tag{1}$$

where $p(\boldsymbol{X})$ is set to a normal distribution where the mean $\mu = 0$ and variance σ_S^2. T in the AWGN is expressed as

$$T = \frac{1}{2}\log_2\left(1 + \frac{\sigma_S^2}{\sigma_N^2}\right). \tag{2}$$

Let σ_N^2 be the noise power and σ_S^2 be the average power of $\boldsymbol{X}$. Equation (2) is the Shannon theorem [21], which indicates the maximum transmission capacity that can be transmitted in AWGN with σ_N^2. Although the Shannon theorem shows that there are coding schemes to achieve T with as low an error rate as possible, it does not specify how to achieve them.

The transmission to satisfy the Shannon theorem can be achieved if the probability distribution of the occurrence of $\boldsymbol{X}$ has a normal distribution. However, it cannot be achieved in practical systems because symbols with extremely high power need to be generated although the probability of their occurrence is extremely low. Therefore, multi-level modulation, such as M-APSK and M-QAM, is widely adopted as the transmission scheme with efficient spectrum utilization under the power constrained condition. Let M be the modulation multi-level number, where $M = 2^n$ ($n \in \mathbb{N}$). In the practical system in which the transmission power is constrained by multi-level modulation, M symbols are generated with uniform probability, that is, $p(\boldsymbol{X}) = 1/M$ and T in AWGN is given as

$$T = \log_2 M - \frac{1}{M}\sum_{i=0}^{M-1}\int_{-\infty}^{\infty} p(\boldsymbol{y}|\boldsymbol{x_i})\log_2\left\{\frac{\sum_{k=0}^{M-1} p(\boldsymbol{y}|\boldsymbol{x_k})}{p(\boldsymbol{y}|\boldsymbol{x_i})}\right\}d\boldsymbol{y} \tag{3}$$

$$p(\boldsymbol{y}|\boldsymbol{x_i}) = \frac{1}{\sqrt{2\pi\sigma_N^2}}exp\left(-\frac{|\boldsymbol{y}-\boldsymbol{x_i}|^2}{2\sigma_N^2}\right) \tag{4}$$

$$\boldsymbol{x_i} = I_i + jQ_i \tag{5}$$

The notation $\boldsymbol{x_i}$ denotes the i-th element of $\boldsymbol{X}$, which is provided in (5) by the i-th in-phase (I_i) and quadrature (Q_i) component of the complex transmission symbol. The notation $\boldsymbol{y}$ denotes the received symbol via the AWGN channel. The transition probability density function $p(\boldsymbol{y}|\boldsymbol{x_i})$, given in (4), is the conditional probability distribution in which the received symbol is identified as $\boldsymbol{y}$ when $\boldsymbol{x_i}$ has been transmitted.

Hence, we used T defined in (3) to design our SP-64APSK coded modulation. The T depends on the parameters M, σ_N^2, and $\boldsymbol{x_i}$. When M is set to 64 and the received carrier-to-noise ratio (C/N) is fixed, that is, σ_N^2 is set to a fixed value, T is regarded as a function of $\boldsymbol{x_i}$. The second part of (3) represents equivocation of whether $\boldsymbol{y}$ is correctly recognized as $\boldsymbol{x_i}$ or other symbols when $\boldsymbol{x_i}$ has been transmitted. As the D_{min} between each adjacent $\boldsymbol{x_i}$ becomes smaller, the probability of receiving $\boldsymbol{x_i}$ correctly becomes lower; consequently, equivocation becomes larger and T decreases. Therefore, maximizing T contributes to the increase in the D_{min} between each adjacent $\boldsymbol{x_i}$. We use T as the criterion of designing the constellation and SP-applicable bit allocation.

B. Constellation

Since the general constellation of APSK modulation is configured to place symbols on multiple concentric circles, there are numerous possible constellation patterns depending on how the constellation symbols are arranged on the IQ plane. We thus set design conditions *1)* to *5)* and parameters *a)* to *c)* shown below and in Fig. 2. These design parameters are determined in the order of *a)* to *c)* so that T is maximized. Design conditions *1)* and *2)* are set to design a symmetric constellation in consideration of the use of an ISDB-S3-compliant pilot signal [4]–[6] which has the same modulation scheme as the main signal modulation to estimate the reference constellation points. Design condition *4)* is determined so that error-free transmission can be achieved at a C/N with a margin of about 1 dB from the theoretical limit C/N of 14.9 dB for DVB-S2X's 64APSK modulation with a coding rate of 4/5.

<Design conditions>

1) Constellation symbols are placed on each of all four circles at equal intervals.

2) The number of constellation symbols placed on each circle is even.

3) The average power should be 1.

4) C/N is 16 dB.

5) Coding rate of 4/5.

<Design parameters>

a) Number of constellation symbols placed on each circle (p_1-p_4) $\sum_{i=1}^{4} p_i = 64$

b) Constellation-symbol phases (θ_1-θ_4) Phases between the I axis and the constellation symbols closest to the I axis are defined as θ_1-θ_4, and each phase is varied in steps of 0.1 degree starting from the initial angles π/p_1 - π/p_4, respectively.

c) Radius ratios between circles (γ_1-γ_3) Radii of the 1st-4th circles are r_1-r_4. Radius ratios are defined as $\gamma_1 = r_2/r_1$, $\gamma_2 = r_3/r_1$, $\gamma_3 = r_4/r_1$, and each one is varied in the ranges of 1.5 to 2.5, 2.5 to 3.5, and 3.5 to 4.5 in steps of 0.01, respectively.

Under these design conditions and design parameter a), there are 4,495 candidates for the 64APSK constellation. After determining *a)* from these candidates, in the order of *b)* and *c)*,

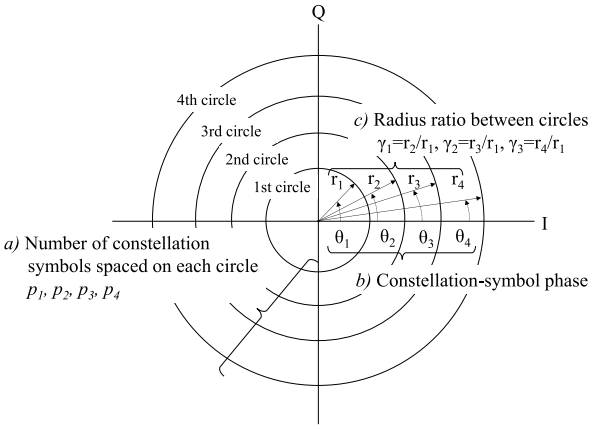

Fig. 2. Constellation design parameters.

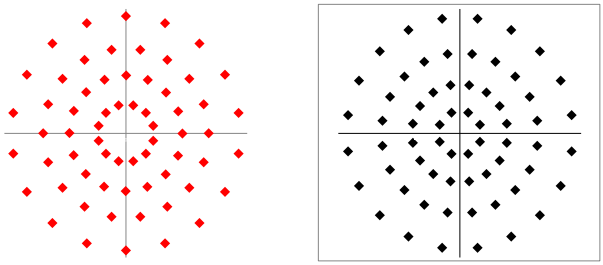

(a) Our 64APSK (12, 16, 18, 18)

(b) DVB-S2X's 64APSK (8, 16, 20, 20)

Fig. 3. Constellations of designed 64APSK and DVB-S2X's 64APSK.

TABLE I
64APSK CONSTELLATIONS

Design parameters	Our 64APSK	DVB-S2X's 64APSK
T [bps/Hz]	5.0839	5.0806
No. of constellation symbol (p_1-p_4)	(12,16,18,18)	(8,16,20,20)
Phase (θ_1-θ_4) [deg.]	(15, 22.25, 0, 10)	(22.25, 11.25, 9.0, 9.0)
Radius ratio (γ_1-γ_3)	(2.00, 2.93, 4.05)	(2.2, 3.6, 5.2)

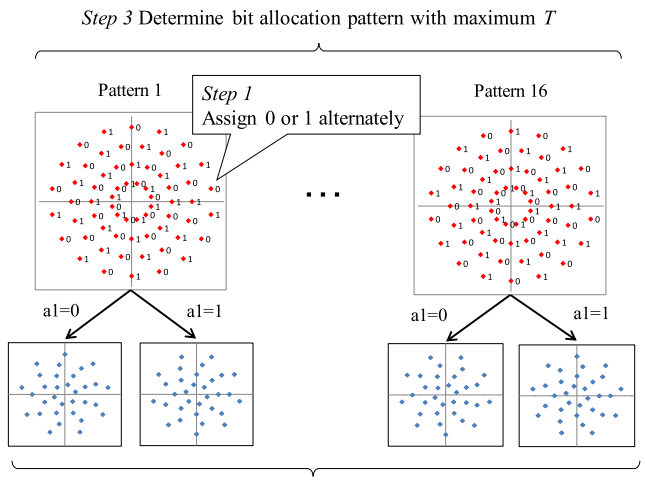

Fig. 4. Developed bit-allocation method.

we determined a 64APSK constellation in which T was maximized as much as possible among the candidates by varying the design parameters through computer simulation [15], [16]. Table I shows the determined values of the parameters for the 64APSK we designed. To confirm whether our 64APSK also has high noise immunity, the values for the 64APSK of DVB-S2X are also indicated in the table as a benchmark, although that of DVB-S2X is designed based on BICM capacity. Fig. 3 illustrates respective constellations. As indicated in Table I, the T of our designed 64APSK achieved 5.0839 bps/Hz, which is larger than that of DVB-S2X.

C. Bit Allocation and Error-Correction Code

We designed the SP-applicable bit allocation to our 64APSK constellation and an error-correction code for each bit. As described below, it is possible to design an SP-64APSK coded modulation with high noise immunity by designing a combination of bit allocation and error-correction codes. Let the six-bit allocation to the 64APSK constellation be (a1, a2, a3, a4, a5, a6). Since the received 64APSK constellation is decoded and divided into 32APSK, 16APSK, . . . , and BPSK in order in

accordance with the decoding results of the previous bits, the constellations on each dividing stage should also have as large a T as possible to increase the robustness to AWGN. We thus determined the bit allocation to the 64APSK constellation using T on each dividing stage as the evaluation function.

The error-correction code is the concatenated code composed of shortened BCH code [22] (65535, 65167) with the correction ability of 23 bits and LDPC code compliant with ISDB-S3.

There are 64! (approx. 1×10^{89}) patterns for assigning a 6-bit sequence (a1, a2, . . . , a6) to each of the 64 symbols, and it is not practical to calculate T for all patterns and find the pattern with the largest T. Therefore, we developed a method for efficient allocation for our 64APSK constellation. Our bit-allocation method is illustrated in Fig. 4 for a1 as an example. The procedure is as follows.

Step 1: Bit of 0 or 1 are alternately assigned to each four circles independently. This enables even dispersal of symbols after division and expansion of the Euclidean distance between symbols. There are $2^4 = 16$ allocation patterns.

Step 2: Our 64APSK constellation is divided into 32APSK constellations in accordance with the assigned a1 $=$ 0 or 1, then the Ts of the divided 32APSK constellations, $M = 32$ in (3), are calculated for 16 patterns. The C/N is set to 16 dB.

Step 3: The bit-allocation pattern for a1 with the largest T in the 16 patterns is determined.

By repeating steps 1 to 3 in the same manner, the bit allocation for a2 to a6 is determined using each T of the divided 16APSK, 8PSK, QPSK, and BPSK constellations. Let the bit allocation designed in steps 1 to 3 be (a1', a2', a3', a4', a5', a6').

Fig. 5 shows the C/N vs. BER characteristics before error-correction for a1' to a6', and Table II lists the BERs at a C/N of 16 dB. We set raw BER range in which it is possible to design appropriate LDPC code compliant with ISDB-S3 to

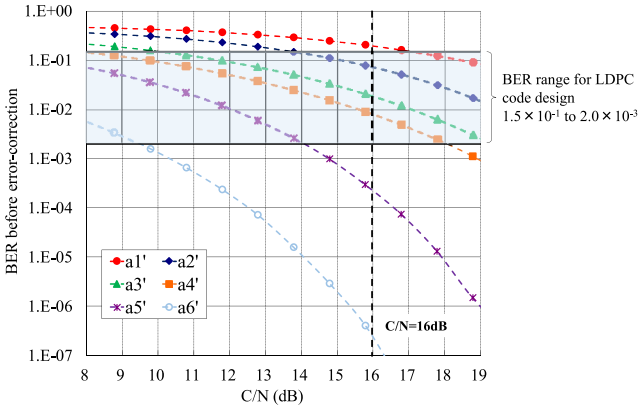

Fig. 5. BER characteristics for each bit.

TABLE II
BER FOR EACH BIT

Bit	BER at C/N of 16 dB
a1'	1.96×10^{-1}
a2'	7.18×10^{-2}
a3'	1.86×10^{-2}
a4'	8.06×10^{-3}
a5'	2.17×10^{-3}
a6'	2.67×10^{-7}

achieve error-free transmissions. Outside the raw BER range of 1.5×10^{-1} to 2.0×10^{-3}, it is difficult to design an LDPC code with a very low or high coding rate while maintaining randomness and high error-correction capability. Table II indicates that the BERs of a1', a5' and a6' are out of this range.

The BER of a6' is less than 1.2×10^{-4}, which can be error-free by only the BCH code and the LDPC code is not needed. Therefore, the bit position of a6' is left unchanged, and the positions of a1' to a5' are shifted, such as a2', a1', a4', a3', a5', to adjust the BER characteristics for each bit so that these BERs fall in the above range.

We calculated the BER for each of the various shifts of a1' to a5' and finally determined the bit allocation (a2', a1', a4', a5', a3', a6') as (a1, a2, a3, a4, a5, a6). Fig. 6 shows the C/N vs. BER characteristics before error-correction for a1 to a6. Table III lists the BERs at a C/N of 16 dB and the LDPC coding rates (Rs) applied to a1 to a5. The BERs of a1 to a5 are in the BER range from 1.5×10^{-1} to 2.0×10^{-3} as a result of shifting the bit positions. The Rs are determined from the BERs for each bit and the average R for a1 to a6 is 4/5. Fig. 7 illustrates the LDPC blocks for each bit, designed to be compliant with ISDB-S3 and with the coding rates indicated in Table III. Fig. 8 shows the final bit allocation and the constellation partitioning results in accordance with Dec_a1 of 0 or 1. We express the six bits allocated to each symbol of the constellation in octal notation (e.g., 26 = 010:110), and the first bit a1 and sixth bit a6 are defined as MSB and LSB, respectively.

D. Computer Simulation Result

Fig. 9 shows the computer simulation results of the C/N vs. BER characteristics after error correction in AWGN. It was

TABLE III
LDPC CODING RATES AND BER FOR EACH BIT

Bit	R	BER at C/N of 16 dB
a1 (a2')	55/120	1.39×10^{-1}
a2 (a1')	65/120	1.13×10^{-1}
a3 (a4')	105/120	1.93×10^{-2}
a4 (a5')	114/120	4.57×10^{-3}
a5 (a3')	117/120	2.84×10^{-3}
a6 (a6')	120/120	2.67×10^{-7}

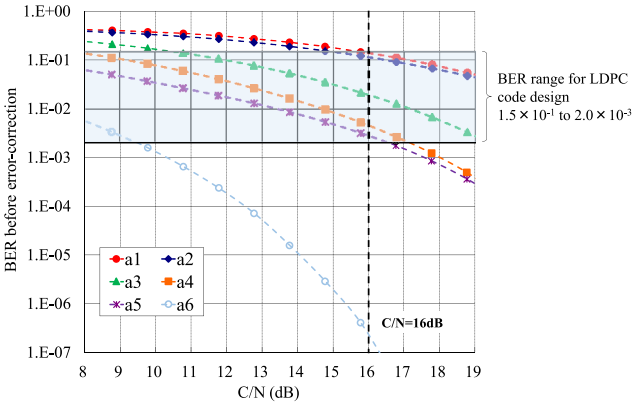

Fig. 6. BER characteristics for each bit after bit-position shift.

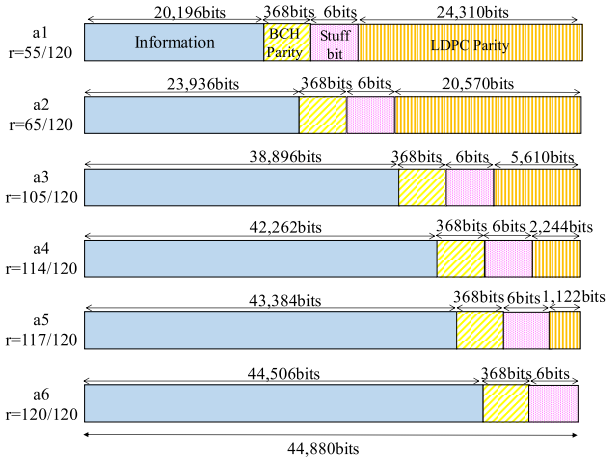

Fig. 7. LDPC blocks for each bit compliant with ISDB-S3.

calculated for our SP-64APSK coded modulation and DVB-S2X's 64APSK modulation with the LDPC coding rate of 4/5 in order to verify our performance by comparing that of DVB-S2X as a benchmark. The concatenated code composed of shortened BCH code (65535, 65167) and LDPC code with code length 44,880 bits was applied to our SP-64APSK coded modulation, and that of BCH code (51840, 51648) and LDPC code with 64,800 bits and the bit interleaver specified in [19], [23] was applied to DVB-S2X's 64APSK. The BERs were calculated in the range of 10^{-8} to 10^{-10}, and the C/N at BER = 1×10^{-11}, which is defined as the required C/N, was obtained by linear extrapolation from the BER calculation results [6]. Since the ISDB-S3 compliant LDPC and BCH code guarantee that there is no error floor even at BER = 1×10^{-11} [4], the extrapolation was used in the BER

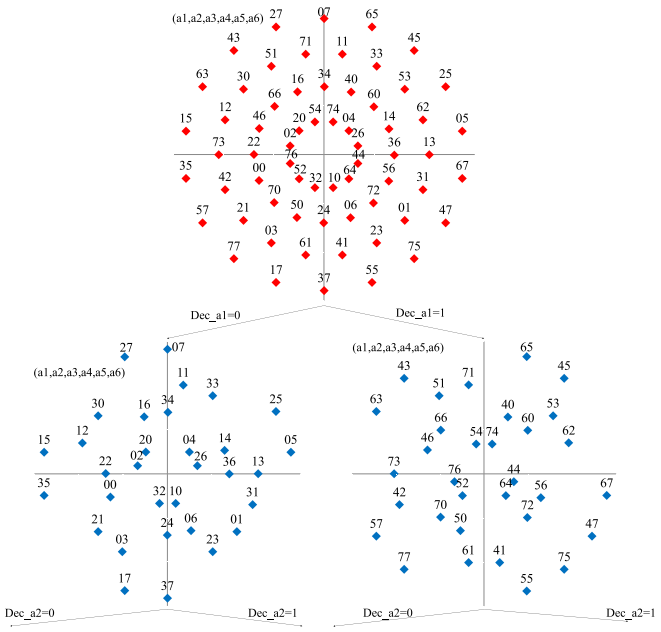

Fig. 8. Final bit allocation and constellation partitioning results.

TABLE IV
SPECIFICATIONS OF PROTOTYPE TRANSMITTER AND RECEIVER

Modulation scheme		SP-64APSK coded modulation
Symbol rate		30.0-34.4 Mbaud
Roll-off factor		0.01-0.35
Number of filter taps		Transmitter: 1024 Receiver: 512
Error-correction code	Outer code	shortened BCH code (65535, 65167, t=23)
	Inner code	LDPC code with coding rate of 4/5 (code length 44880 bits)
LDPC decoding algorithm		min-sum decoding [24]
Non-liner compensation		Pilot signal with 64APSK constellation
Maximum bit rate		158.6 Mbps

calculation. Error propagation which was concerned in SP-multi-level coded modulation did not occur. The required C/N of our SP-64APSK coded modulation is 15.70 dB [15], which is 0.36 dB lower than that of DVB-S2X's 64APSK modulation with the same LDPC coding rate. We confirmed that our SP-64APSK coded modulation could achieve better transmission performance than the modulation scheme with Gray mapping by applying an error-correction code with proper capability for each bit in accordance with the constellation partitioning. While our SP-64APSK coded modulation scheme has a concern to increase latency and complexity than the modulation scheme with BICM and Gray mapping, we verify in the next section that they are at acceptable levels for our prototype implementation.

IV. Development of Transmitter and Receiver

A. Specifications

We prototyped a transmitter and receiver that can implement our SP-64APSK coded modulation scheme. Table IV lists the

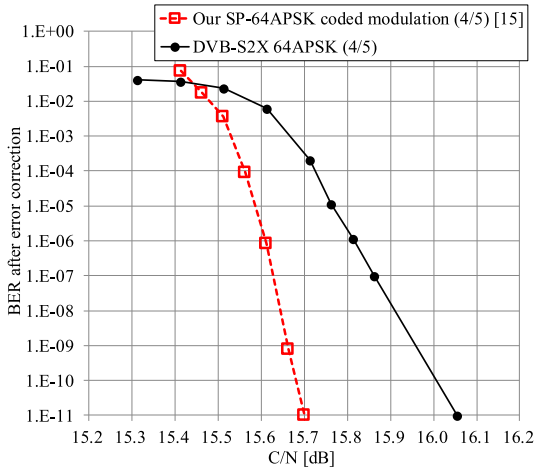

Fig. 9. C/N vs. BER characteristics after error-correction.

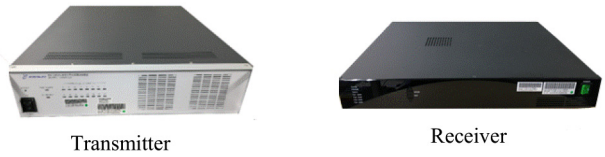

Fig. 10. Photos of prototype.

specifications and Fig. 10 shows the photos of the prototype. The min-sum decoding algorithm [24] for LDPC is used in the prototype. The maximum number of LDPC decoding iterations is set to 50.

The prototype is equipped with a mechanism to know the effect of non-linear distortion caused by the satellite transponder by using the pilot signal, which is a known 64APSK constellation symbol. At the receiver side, the log likelihood ratio (LLR) is calculated using the pilot signal as a reference point to reduce the degradation of LDPC decoding performance due to non-linear distortion [4]–[6]. The maximum transmission rate of the prototype is 158.6 Mbps with an LDPC coding rate of 4/5 and symbol rate of 34.4 Mbaud.

B. Transmitter

Fig. 11 illustrates a block diagram of the transmitter, focusing on the structure of the main signal. Transmitted bit streams are error correction encoded in the order from a1 to a6 in accordance with the LDPC block structure shown in Fig. 7. Each LDPC block is called a "slot". The transmitter works in units of 24 fundamental frames (FFs) composed of sets of 6 slots (#1 to #6, #7 to #12, . . . , #139 to #144).

The bits in an FF are mapped to the 64APSK constellation, and the symbols are input to the modulation frame (MF)-structure section shown in Fig. 12. An MF consists of the modulation symbol for the main signal (64APSK), transmission and multiplexing configuration control (TMCC), pilot signal, and synchronization signal. It has 120 modulation slots (MSs), with which our SP-64APSK coded modulation scheme can be implemented to the existing ISDB-S3 transmitter without major changes. "Data" in Fig. 12 denotes a portion of the 64APSK symbol modulated in the main-signal section

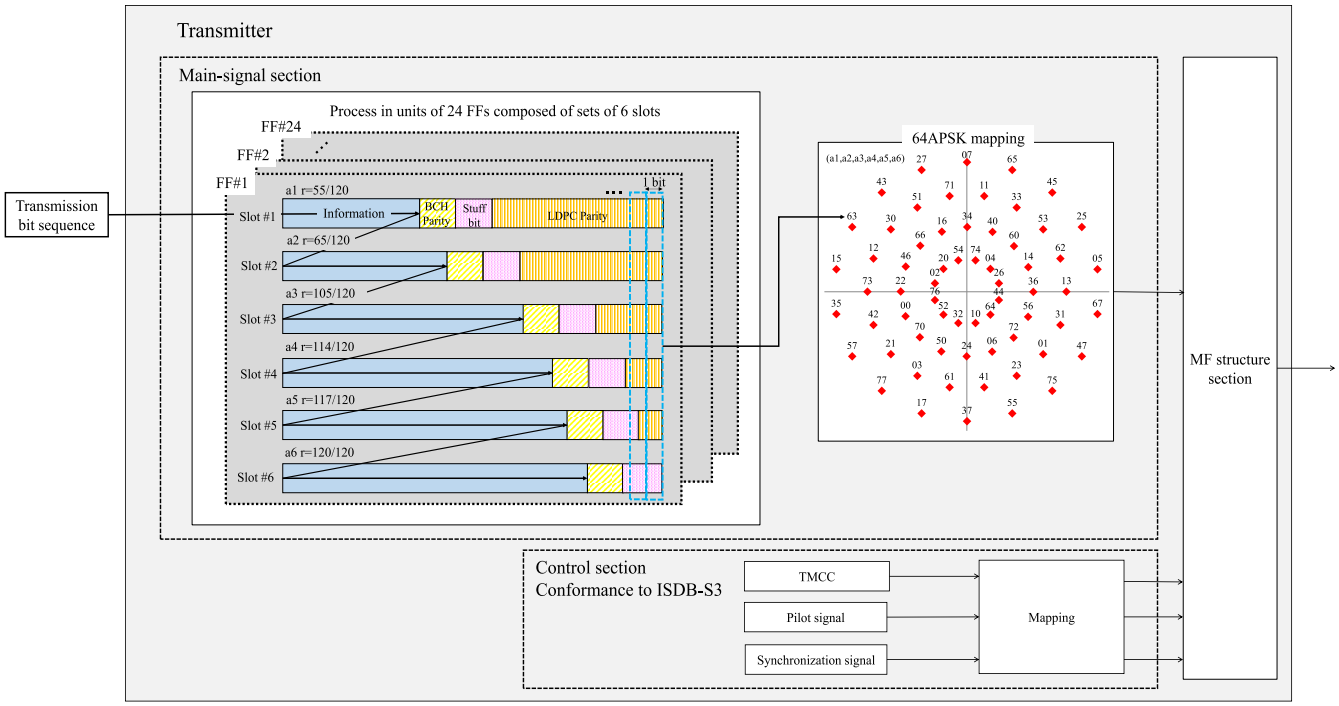

Fig. 11. Block diagram of transmitter focusing on frame structure of main-signal.

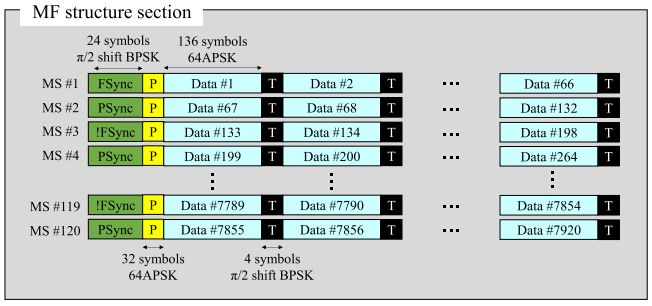

Data : 64APSK symbols modulated in main signal unit
P : Pilot signal
T : TMCC signal
Fsync,!Fsync : Frame synchronization signal (! indicates bit inversion)
Psync : Slot-synchronization signal

Fig. 12. MF-structure section.

described in Fig. 11 and has 136 symbols each. Since one MS has 66 "Data", the total number of symbols in an MF is 1,077,120 (=136 symbols × 66 × 120), which corresponds to 6,462,720 bits (=1,077,120 × 6) for 64APSK modulation. Operating the transmitter in 24 FFs composed of sets of 6 slots (24 FFs×6 slots×44,880 bits = 6,462,720 bits) results in being 120 MSs in an MF structure, and it is possible to apply the MF of ISDB-S3, which specifies up to 32APSK, to 64APSK.

A pilot signal consisting of 64 symbols of 64APSK is transmitted using two MSs, because one MS has 32 symbols for the pilot signal. The first 32 symbols corresponding to the bit sequences for "000000", "000001", . . . , "011111" are transmitted in the odd-MS and the second 32 symbols corresponding to the bits for "100000", "100001", . . . , "111111" are in the even-MS in order by which the pilot signal can be transmitted 60 times per MF.

C. Receiver

Fig. 13 illustrates the block diagram of the receiver, focusing on the multi-level decoding process. This process is as follows.

a) The IQ signals of 44,880 symbols obtained by orthogonal demodulation are read from IQ memory, and their LLRs for a1 (LLR_a1) are calculated at the uppermost part of the LLR-calculation section in Fig. 13 in accordance with the 64APSK reference IQ. When the pilot signal is used for non-linear distortion compensation, each reference IQ is replaced with the pilot signal IQ that is transmitted periodically as described in Section IV-B and averaged on the receiver [4].

b) LLR_a1 are sent to the LDPC-decoder section and decoded with the parity check matrix (PCM) for a1 by the min-sum decoding algorithm of LDPC. The LDPC-decoded bits for a1 are then decoded by the BCH decoder, and the result (Dec_a1) is stored in the decoded bit memory. Dec_a1 is fed back to the "reference IQ select SW" in the LLR-calculation section for a2 decoding.

c) LLR for a2 (LLR_a2) is calculated from the IQ signal and the 32APSK reference IQ selected by the switch (SW) on the basis of each decoded bit of a1 (Dec_a1). When the decoded bit in a1 is 0, the 32APSK constellation for Dec_a1 = 0 is selected, when it is 1, the one for Dec_a1 = 1 is used for the reference symbol point. When the pilot signal is used, it is the same as a1.

d) LLR_a2 are sent to the LDPC-decoder section and decoded with PCM for a2. The LDPC-decoded bits for a2 are then decoded with the BCH decoder (Dec_a2) and stored in the decoded bit memory. Dec_a1 and Dec_a2 are fed back to the SW for a3 decoding.

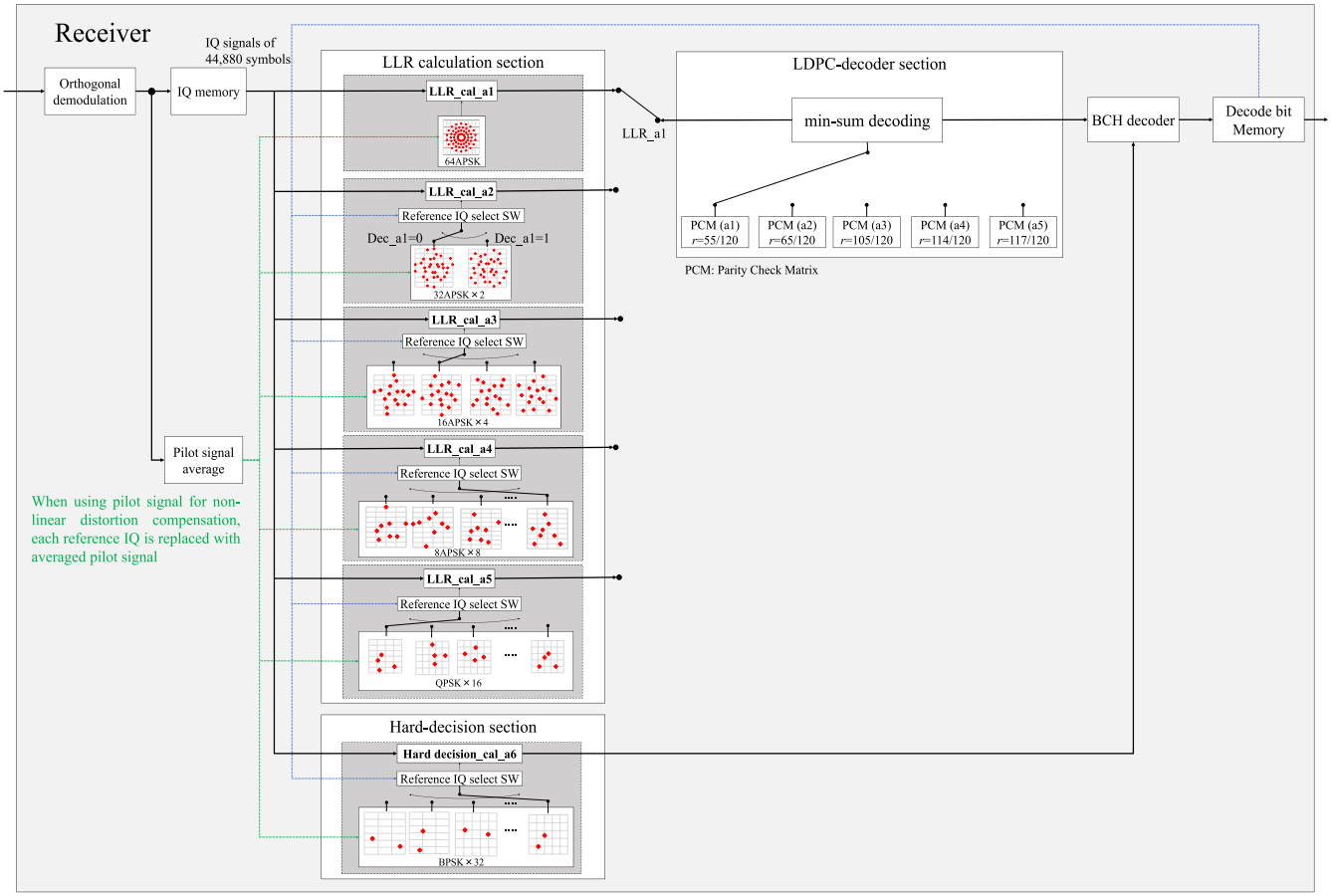

Fig. 13. Multi-level decoding process in receiver.

e) Repeat steps from *c)* to *d)* for decoding a3 to a5 in the same manner using the constellations from 16APSK to QPSK respectively to calculate the LLRs. Since a6 does not require an LDPC decoding, the hard-decision-decoded bit sequence is input to the BCH decoder. The reference IQ for the hard-decision decoding for a6 is selected from 32 BPSK constellations in accordance with all the bits from Dec_a1 to Dec_a5 by the reference IQ-select SW.

V. Transmission-Performance Evaluation of Prototype

A. Performance in AWGN Channel

We evaluated the transmission performance of the prototype in AWGN with modulation parameters set to a symbol rate of 33.7561 Mbaud and roll-off factor of 0.03, which are used in 4K/8K UHDTV satellite broadcasting in Japan [4]. We measured the BER performance by adding AWGN and found the required C/N in the experimental system illustrated in Fig. 14. The required C/N for the prototype (C/N_{pro}) in AWGN was 16.6 dB. Since that in the computer simulation (C/N_{sim}) [15] was 15.7 dB, we confirmed that the prototype could achieve error-free transmission with the required C/N degradation within about 1.0 dB compared with the result of the computer simulation in AWGN. The 0.9 dB difference between them is considered to be the degradation in transmission performance due to hardware processing. To analyze the breakdown of the 0.9 dB difference, we measured the modulation error ratio (MER) [25], which is the ratio of ideal symbol power to error power that is the difference between the ideal symbol and demodulated symbol, when the transmitter and receiver were directly connected (loop back) without adding AWGN. The amount of noise generated in the device can be estimated from the MER. The MER was 29.2 dB in the loop back, and the constellation is shown on the left side in

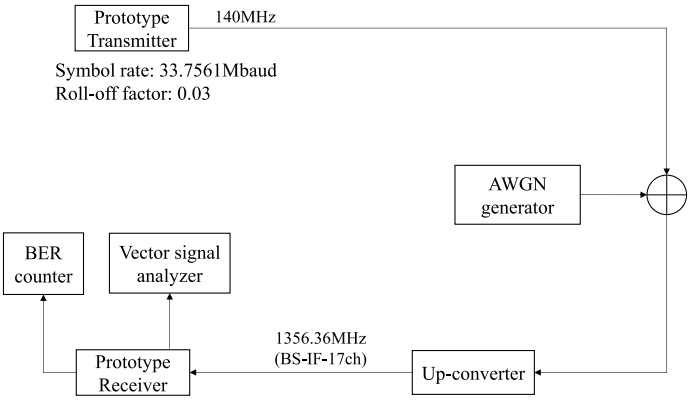

Fig. 14. Experimental system for measuring BER performance in AWGN.

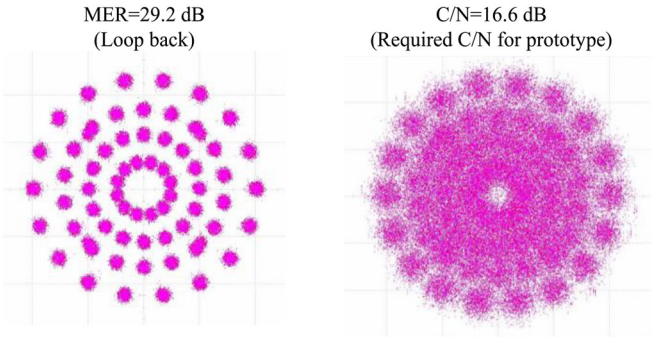

Fig. 15. Received constellations.

Fig. 15. There were implementation losses due to FIR filters and internal noise in the prototype. Because of these losses, each received constellation symbol did not converge to a single point, unlike in the computer simulation.

$$C/N_{loop} = 10\log\left\{\frac{1}{\left(10^{-\frac{C/N_{\rm sim}}{10}}\right) - \left(10^{-\frac{MER}{10}}\right)}\right\}\ [dB] \quad (6)$$

The required C/N of the prototype with the loop back connection (C/N_{loop}) including the implementation losses can be obtained from (6), and 15.9 dB is obtained from $C/N_{\rm sim}$ (15.7 dB) and MER (29.2 dB). Therefore, the 0.9 dB gap is considered composed of 0.2 dB ($= C/N_{loop} - C/N_{\rm sim}$) due to the hardware implementation and 0.7 dB due to the LDPC decoding process in the prototype. While the sum-product algorithm [26] was used in the computer simulation, the min-sum decoding algorithm [24], which approximates the tanh function (an update expression for check-node) with the minimum function, was used for the LDPC decoding in the prototype. The min-sum decoding algorithm is easier to implement in hardware than the sum-product algorithm, but its decoding accuracy is inferior to that of the sum-product algorithm, and it is considered to be the main cause of degradation in the LDPC decoding process in the prototype.

B. Performance in Non-Linear Channel Simulating 12-GHz-Band Satellite Transponder Characteristics

We also evaluated the transmission performance of the prototype in the non-linear channel simulating 12-GHz-band satellite transponder characteristics [27]. Fig. 16 illustrates the experimental system with the 12-GHz-band satellite simulator [28], which consists of input/output multiplexer (IMUX/OMUX) filters with a center frequency of 12.03436 GHz and bandwidth of 34.5 MHz, a traveling wave tube amplifier (TWTA) without a linearizer, and variable attenuation to adjust the output back-off (OBO) [29] of the TWTA. The AM-AM and AM-PM characteristics of the TWTA are shown in Fig. 17. The frequency amplitude and group delay characteristics of the IMUX/OMUX filters are shown in Fig. 18. The transmission parameters of the prototype were the same as those mentioned in Section V-A and the pilot signal was used for non-linear compensation. The

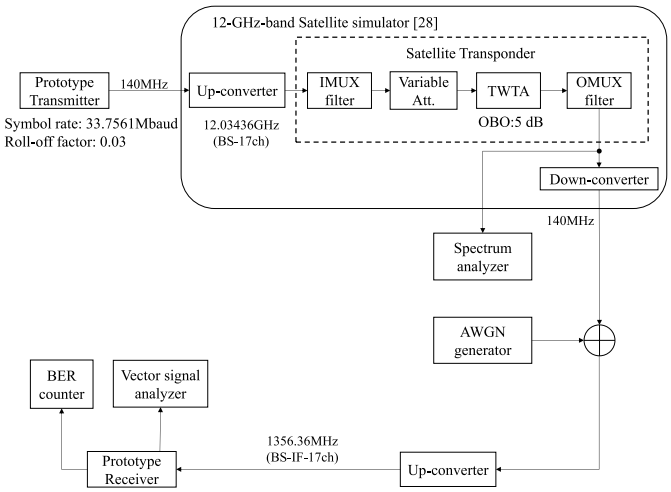

Fig. 16. Experimental system including 12-GHz-band satellite simulator.

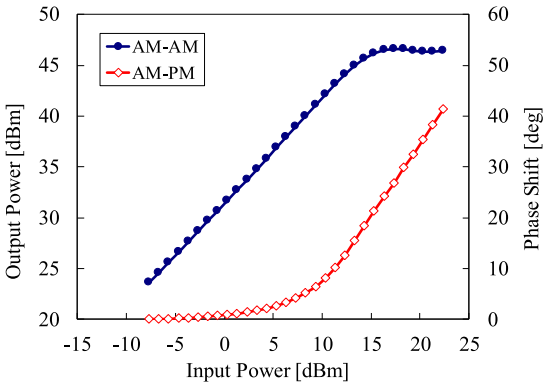

Fig. 17. AM-AM and AM-PM characteristics of TWTA (center frequency: 12.03436 GHz).

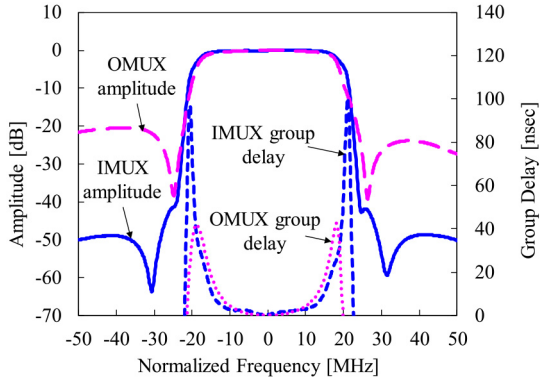

Fig. 18. Frequency amplitude and group delay characteristics of IMUX/OMUX filter (center frequency 12.03436 GHz is normalized to 0 Hz).

received C/N was set by adding white noise with an AWGN generator.

The OBO is an important parameter to evaluate transmission performance through a satellite transponder because it is related to the amount of non-linear distortion occurring in the TWTA. We define the OBO of the modulated signal as the ratio of the saturated maximum output power of a continuous wave to the operation output power of the modulated signal [28]. The optimal OBO for multi-level modulation

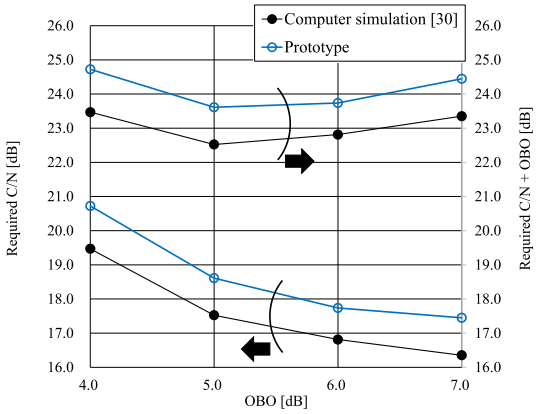

Fig. 19. OBO vs. required C/N + OBO characteristics.

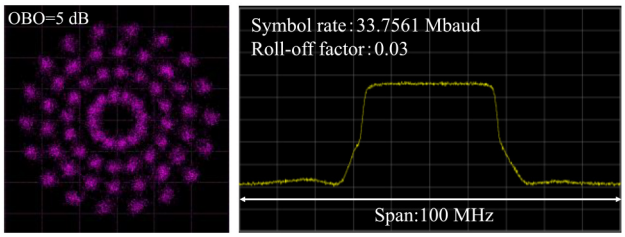

Fig. 20. Constellation and spectrum of received signal through non-linear channel at OBO = 5 dB without AWGN (center frequency: 12.03436 GHz).

transmission can be obtained when the required C/N + OBO is a minimum [28].

Fig. 19 plots the OBO vs. required C/N (right vertical line) and required C/N + OBO (left vertical line) characteristics of the prototype in the non-linear channel. It also shows the computer-simulation results from a previous study [30] calculated under the same condition. The optimal OBO for our SP-64APSK coded modulation in the hardware experiment was 5 dB, which agreed with the computer simulation. Fig. 20 shows the received constellation and spectrum. The required C/N for the prototype in the non-linear channel set to OBO of 5 dB was 18.6 dB and the performance difference between the computer simulation [30] and prototype was 1.1 dB.

C. Performance Summary

We summarize the transmission performance of the prototype in the AWGN and non-linear channels when the OBO was set to 5 dB described in Sections V-A and V-B. Fig. 21 shows the BER characteristics of the prototype and computer simulation [15], [30]. The required C/Ns of the prototype in AWGN and non-linear channel are 16.6 and 18.6 dB, and those of the computer simulation in both channels were 15.7 and 17.5 dB, respectively. The required C/N degradation from the computer simulated values due to the implementation of our SP-64APSK coded modulation was about 1 dB in both channels. The degradation due to the non-linear channel was 1.8 dB in the prototype and 2.0 dB in the simulation. These results confirm that the prototype has similar performance estimated from the computer simulation in both channels.

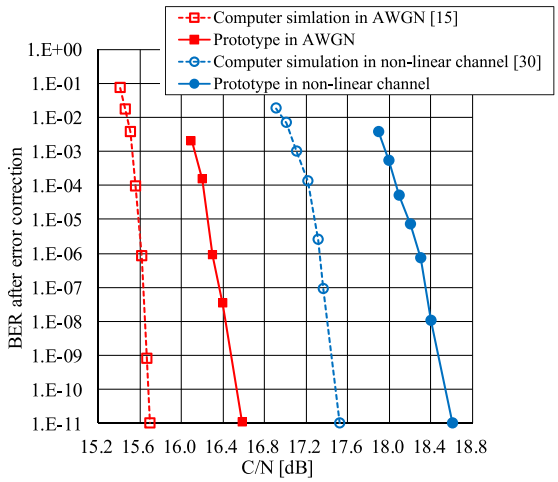

Fig. 21. Summary of transmission performance in AWGN and non-linear channels.

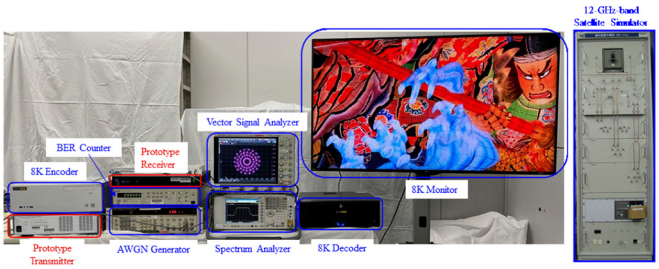

Fig. 22. Photo of 8K UHDTV transmission experiment.

D. 8K UHDTV Transmission

We conducted an 8K UHDTV transmission with the prototype and the 12-GHz-band satellite simulator in the experimental system shown in Fig. 16. The transmission parameters and satellite simulator's settings were the same as those in Sections V-A and V-B, respectively. The OBO was set to 5 dB. The 8K UHDTV was encoded to 150 Mbps by High Efficiency Video Coding (HEVC) [31], [32], and its container format used the MPEG2-TS system. The received C/N was varied by adding AWGN to measure the detection limit of the C/N, which was defined as the minimum received C/N at which no block noise occurred during a one-minute viewing of the transmitted 8K UHDTV video.

A photo of the 8K UHDTV transmission experiment is shown in Fig. 22. We confirmed that 8K UHDTV with an encoded bit rate of 150 Mbps could be transmitted using the prototype with our SP-64APSK coded modulation in the non-linear channel. The detection limit C/N was 18.8 dB, which agreed with the C/N vs. BER characteristics mentioned in Section V-B.

VI. Conclusion

We proposed a SP-64APSK coded modulation and developed a prototype transmitter and receiver that can implement the SP-64APSK coded modulation. We outlined the SP-multi-level coded modulation and described our SP-64APSK

TABLE V
IQ COORDINATES AND BIT ALLOCATION

i	I_i	Q_i	a1	a2	a3	a4	a5	a6	Octal
1	0.3369	0.0903	0	1	0	1	1	0	26
2	0.2467	0.2467	0	0	0	1	0	0	04
3	0.0903	0.3369	1	1	1	1	0	0	74
4	-0.0903	0.3369	1	0	1	1	0	0	54
5	-0.2467	0.2467	0	1	0	0	0	0	20
6	-0.3369	0.0903	0	0	0	0	1	0	02
7	-0.3369	-0.0903	1	1	1	1	1	0	76
8	-0.2467	-0.2467	1	0	1	0	1	0	52
9	-0.0903	-0.3369	0	1	1	0	1	0	32
10	0.0903	-0.3369	0	0	1	0	0	0	10
11	0.2467	-0.2467	1	1	0	1	0	0	64
12	0.3369	-0.0903	1	0	0	1	0	0	44
13	0.6457	0.2642	0	0	1	1	0	0	14
14	0.4954	0.4911	1	1	0	0	0	0	60
15	0.2698	0.6434	1	0	0	0	0	0	40
16	0.0030	0.6976	0	1	1	1	0	0	34
17	-0.2642	0.6457	0	0	1	1	1	0	16
18	-0.4911	0.4954	1	1	0	1	1	0	66
19	-0.6434	0.2698	1	0	0	1	1	0	46
20	-0.6976	0.0030	0	1	0	0	1	0	22
21	-0.6457	-0.2642	0	0	0	0	0	0	00
22	-0.4954	-0.4911	1	1	1	0	0	0	70
23	-0.2698	-0.6434	1	0	1	0	0	0	50
24	-0.0030	-0.6976	0	1	0	1	0	0	24
25	0.2642	-0.6457	0	0	0	1	1	0	06
26	0.4911	-0.4954	1	1	1	0	1	0	72
27	0.6434	-0.2698	1	0	1	1	1	0	56
28	0.6976	-0.0030	0	1	1	1	1	0	36
29	0.9833	0.3579	1	1	0	0	1	0	62
30	0.8016	0.6726	1	0	1	0	1	1	53
31	0.5232	0.9063	0	1	1	0	1	1	33
32	0.1817	1.0306	0	0	1	0	0	1	11
33	-0.1817	1.0306	1	1	1	0	0	1	71
34	-0.5232	0.9063	1	0	1	0	0	1	51
35	-0.8016	0.6726	0	1	1	0	0	0	30
36	-0.9833	0.3579	0	0	1	0	1	0	12
37	-1.0464	0.0000	1	1	1	0	1	1	73
38	-0.9833	-0.3579	1	0	0	0	1	0	42
39	-0.8016	-0.6726	0	1	0	0	0	1	21
40	-0.5232	-0.9063	0	0	0	0	1	1	03
41	-0.1817	-1.0306	1	1	0	0	0	1	61
42	0.1817	-1.0306	1	0	0	0	0	1	41
43	0.5232	-0.9063	0	1	0	0	1	1	23
44	0.8016	-0.6726	0	0	0	0	0	1	01
45	0.9833	-0.3579	0	1	1	0	0	1	31
46	1.0464	0.0000	0	0	1	0	1	1	13
47	1.3741	0.2423	0	0	0	1	0	1	05
48	1.2083	0.6976	0	1	0	1	0	1	25
49	0.8969	1.0688	1	0	0	1	0	1	45
50	0.4772	1.3111	1	1	0	1	0	1	65
51	0.0000	1.3953	0	0	0	1	1	1	07
52	-0.4772	1.3111	0	1	0	1	1	1	27
53	-0.8969	1.0688	1	0	0	0	1	1	43
54	-1.2083	0.6976	1	1	0	0	1	1	63
55	-1.3741	0.2423	0	0	1	1	0	1	15
56	-1.3741	-0.2423	0	1	1	1	0	1	35
57	-1.2083	-0.6976	1	0	1	1	1	1	57
58	-0.8969	-1.0688	1	1	1	1	1	1	77
59	-0.4772	-1.3111	0	0	1	1	1	1	17
60	0.0000	-1.3953	0	1	1	1	1	1	37
61	0.4772	-1.3111	1	0	1	1	0	1	55
62	0.8969	-1.0688	1	1	1	1	0	1	75
63	1.2083	-0.6976	1	0	0	1	1	1	47
64	1.3741	-0.2423	1	1	0	1	1	1	67

coded modulation design method consisting of design methods of constellation, bit allocation, and the LDPC code through computer simulation. We used the channel capacity in AWGN and designed the constellation and bit allocation that can maximize it as much as possible. We confirmed that our SP-64APSK coded modulation improves the required C/N in AWGN by about 0.36 dB than that of DVB-S2X's 64APSK modulation through computer simulation. We explained the modulation/demodulation process and transmission performance of the prototype with our SP-64APSK coded modulation and verified that the prototype has similar transmission performance with a difference of about 1 dB than the computer simulation in the AWGN and non-linear channels. We also showed that the prototype could transmit 8K UHDTV with an encoded bit rate of 150 Mbps in the 34.5 MHz bandwidth of a single transponder for satellite broadcasting.

APPENDIX

Table V lists the IQ coordinates of the 64APSK constellation and bit allocation described in Section III-B and C, respectively.

REFERENCES

[1] "Parameter values for ultra-high definition television systems for production and international programme exchange," ITU, Geneva, Switzerland, ITU-Recommendation BT.2020-2, Oct. 2015.

[2] "Image parameter values for high dynamic range television for use in production and international programme exchange," exchange," ITU, Geneva, Switzerland, ITU-Recommendation BT.2100-2, Jul. 2018.

[3] K. Hayashi and K. Kumamaru, S. Yokozawa, "Development of new UHD-1 (4K)/UHD-2 (8K) UHDTV satellite broadcasting system in Japan," *SMPTE Motion Imag. J.*, vol. 129, no.6, pp. 15–24, Jul. 2020.

[4] Y. Suzuki and H. Sujikai, "Transmission system of 4K/8K UHDTV satellite broadcasting," *IEICE Trans. Commun.*, vol. E103-B, no. 10, pp. 1050–1058, Oct. 2020.

[5] "Transmission system for UHDTV satellite broadcasting," ITU, Geneva, Switzerland, ITU-Recommendation BO.2098, Dec. 2016.

[6] *Transmission System For Advancedwide Band Digital Satellite Broadcasting*, ARIB Standard-B44 ver. 2.1-E1, Mar. 2016.

[7] S. Hara, A. Hanada, I. Masuhara, Y. Yamashita, and K. Mitani, "Celebrating the launch of 8K/4K UHDTV satellite broadcasting and progress on full-featured 8K UHDTV in Japan," *SMPTE Motion Imag. J.*, vol. 127, no. 2, pp. 1–8, Mar. 2018.

[8] G. Ungerboeck, "Trellis-coded modulation with redundant signal sets Part I: Introduction," *IEEE Commun. Mag.*, vol. TCM-25, no. 2, pp. 5–11, Feb. 1987.

[9] M. Isaka, M. P. C. Fossorier, R. H. Morelos-Zaragoza, S. Lin, and H. Imai, "Multilevel coded modulation for unequal error protection and multistage decoding. II. Asymmetric constellations," *IEEE Trans. Commun*, vol. 48, no. 5, pp. 774–786, May 2000.

[10] R. Farhoudi and L. A. Rusch, "Multi-level coded modulation for 16-ary constellations in presence of phase Noise," *J. Lightw. Technol.*, vol. 32, no. 6, pp. 1159–1167, Mar. 15, 2014.

[11] M. Tanahashi and H. Ochiai, "A multilevel coded modulation approach for hexagonal signal constellation," *IEEE Trans. Wireless Commun*, vol. 8, no. 10, pp. 4993–4997, Oct. 2009.

[12] Y. Suzuki, A. Hashimoto, Y. Matsusaki, S. Tanaka, T. Kimura, and K. Tsuchida, "The performance improvement of set partitioning 8PSK coded modulation using LDPC and BCH concatenated code," *IEICE Trans.*, vol. J97-B, no. 8, pp. 648–659, 2014.

[13] Y. Suzuki, M. Kojima, Y. Koizumi, M. Kamei, K. Saito, and S. Tanaka, "Set partitioning 16QAM multi-level coded modulation with LDPC codes," in *Proc. 21st Ka Broadband Commun. Conf.*, 2015, p. 301.

[14] Y. Suzuki, Y. Koizumi, M. Kojima, K. Saito, and S. Tanaka, "Set partitioning 32QAM with optimized LDPC coding rates," in *Proc. 22nd Ka Broadband Commun. Conf.*, 2016, p. 7.

[15] Y. Koizumi, Y. Suzuki, M. Kojima, K. Saito, and S. Tanaka, "A study on 64APSK coded modulation," IEICE, Tokyo, Japan, IEICE Rep. SAT2016-55, Oct. 2016.

[16] Y. Koizumi, Y. Suzuki, M. Kojima, K. Saito, and S. Tanaka, "Study on set partitioning 64APSK coded modulation design method based on channel capacity," in *Proc. IEEE Global Commun. Conf.*, 2017, pp. 1–6.

[17] E. Zehavi, "8-PSK trellis codes for a Rayleigh channel," *IEEE Trans. Commun.*, vol. 40, no. 5, pp. 873–884, May 1992.
[18] G. Caire, G. Taricco, and E. Biglieri, "Bit-interleaved coded modulation," *IEEE Trans. Inf. Theory*, vol. 44, no. 3, pp. 927–946, May 1998.
[19] *Digital Video Broadcasting (DVB); Second Generation Framing Structure, Channel Coding and Modulation Systems for Broadcasting, Interactive Services, News Gathecircle and Other Broadband Satellite Applications; Part 2: DVB-S2 Extensions (DVB-S2X)*, ETSI Standard EN 302 307-2 V1.3.1, Jul. 2021.
[20] G. Ungerboeck, "Channel coding with multilevel/phase signals," *IEEE Trans. Inf. Theory*, vol. TIT-28, no. 1, pp. 55–67, Jan. 1982.
[21] C. E. Shannon, "A mathematical theory of communication," *Bell Syst. Techn. J.*, vol. 27, no. 3, pp. 379–423, Jul. 1948.
[22] H. Helgert and R. Stinaff, "Shortened BCH codes," *IEEE Trans. Inf. Theory*, vol. 19, no. 6, pp. 818–820, Nov. 1973.
[23] *Digital Video Broadcasting (DVB); Second Generation Framing Structure, Channel Coding and Modulation Systems for Broadcasting, Interactive Services, News Gathecircle and Other Broadband Satellite Applications; Part 1: DVB-S*, ETSI Standard EN 302 307-1 V1.4.1, Nov. 2014.
[24] J. Zhao, F. Zarkeshvari, and A. H. Banihashemi, "On implementation of min-sum algorithm and its modifications for decoding low-density parity-check (LDPC) codes," *IEEE Trans. Commun.*, vol. 53, no. 4, pp. 549–554, Apr. 2005.
[25] "Methods for objective reception quality assessment of digital terrestrial television broadcasting signals of system B specified in recommendation ITU-R BT.1306," ITU, Geneva, Switzerland, ITU-Recommendation BT.1735-3, Feb. 2015.
[26] D. J. C. MacKay, "Good error-correcting codes based on very sparse matrices," *IEEE Trans. Inf. Theory*, vol. 45, no. 3, pp. 399–431, Mar. 1999.
[27] Y. Koizumi, Y. Suzuki, M. Kojima, and H. Sujikai, "Evaluation of prototype transmitter and receiver with 64APSK coded modulation in non-linear channel," in *Proc. IEEE Int. Conf. Consum. Electron.*, 2019, pp. 1–2.
[28] M. Kojima, M. Nagasaka, Y. Suzuki, Y. Koizumi, K. Saito, and S. Tanaka, "Experimental verification of prototype equalizer for nonlinear compensation over satellite channel," *Trans. Jpn. Soc. Aeronaut. Space Sci. Aerosp. Technol. Jpn.*, vol. 16, no. 3, pp. 248–253, 2018.
[29] M. Aloisio, P. Angeletti, E. Casini, E. Colzi, S. D'Addio, and R. Oliva-Balague, "Accurate characterization of TWTA distortion in multicarrier operation by means of a correlation-based method," *IEEE Trans. Electron Devices*, vol. 56, no. 5, pp. 951–958, May 2009.
[30] Y. Suzuki, Y. Koizumi, M. Kojima, K. Saito, and S. Tanaka, "Nonlinear transmission performance comparison of 64APSK coded modulation with 12-GHz satellite transponder characteristics," in *Proc. 23rd Ka Broadband Commun. Conf.*, 2017, p. 8.
[31] *Information Technology—High Efficiency Coding and Media Delivery in Heterogeneous Environments—Part 2: High Efficiency Video Coding*, Standard ISO/IEC 23008-2, Oct. 2017.
[32] "High efficiency video coding," ITU, Geneva, Switzerland, ITU-T Recommendation H.265, Feb. 2018.

Yuki Koizumi (Member, IEEE) received the B.E. and M.E. degrees in electronic engineering from Tohoku University, Sendai, Japan, in 2010 and 2012, respectively.

He joined Japan Broadcasting Corporation (NHK) in 2012. He has been engaged in research on future satellite broadcasting systems with the Science and Technology Research Laboratories (STRL), NHK since 2015.

Mr. Koizumi is a member of IEICE and ITE.

Yoichi Suzuki (Member, IEEE) received the B.E. and M.E. degrees in electronic engineering from Tohoku University, Sendai, Japan, in 2001 and 2003, respectively.

He has been engaged in research and development and standardization activities for 4K and 8K satellite broadcasting with the Science and Technology Research Laboratories, NHK since 2003. Since 2021, he has been a Senior Manager of the Engineering Administration Department, Japan Broadcasting Corporation (NHK)

Mr. Suzuki is a member of IEICE and ITE.

Masaaki Kojima (Member, IEEE) received the B.E., M.E., and Ph.D. degrees in electrical and electronic engineering from Tokushima University, Tokushima, Japan, in 2000, 2002, and 2015, respectively.

He joined Japan Broadcasting Corporation (NHK) in 2002. He has been engaged in research on further satellite broadcasting systems, millimeter-wave wireless camera systems, and non-linear characteristics of broadcasting satellite transponders with the Science and Technology Research Laboratories, NHK since 2006, where he has been a Principal Research Engineer since 2018.

Dr. Kojima was a recipient of the IEEE CASS Shikoku Chapter Best Paper Award in 2015. He is an Associate Editor of the *IEICE Communications Express*. He is a Senior Member of IEICE and a member of ITE.

Kazunori Yokohata received the B.E. and M.E. degrees in electronic engineering from Hokkaido University, Sapporo, Japan, in 1993 and 1995, respectively.

He joined Japan Broadcasting Corporation (NHK) in 1995. He has been engaged the Broadcast stations, the Engineering Administration Department and Science and Technology Research Laboratories (STRL), NHK. From 2015 to 2018, he was a Deputy Director of the Broadcasting Sattelite System Corporation. From 2018 to 2021, he was a Senior Research Engineer and engaged in research on future satellite broadcasting systems with STRL, NHK. Since 2021, he has been a Chief of the Engineering Division, NHK Asahikawa Station.

Mr. Yokohata is a member of ITE.

Hisashi Sujikai received the B.E. and M.E. degrees in electrical and electronic engineering from Waseda University, Tokyo, Japan, in 1991 and 1993, respectively.

From 2013 to 2017, he was a Senior Manager of the Engineering Administration Department of Japan Broadcasting Corporation (NHK). From 2017 to 2021, he was a Senior Research Engineer and engaged in research on future satellite broadcasting systems with the Science and Technology Research Laboratories, NHK, where he has been a Senior Manager of the Planning and Coordination Division since 2021.

Mr. Sujikai is a Senior Member of IEICE and a member of ITE.